Available online at www.sciencedirect.com
SCIENCE DIRECT®
Journal of Solid State Chemistry 178 (2005) 868–873
JOURNAL OF SOLID STATE CHEMISTRY
www.elsevier.com/locate/jssc

$Sr_{2/3}Y_{1/3}CoO_{8/3+\delta}$: Transition from insulating antiferromagnet to metallic ferromagnet by control of the oxygen content

A. Maignan*, S. Hébert, V. Caignaert, V. Pralong, D. Pelloquin

Laboratoire CRISMAT, UMR 6508 CNRS ISMRA, 6 bd Maréchal Juin, FR-14050 Caen Cedex 4, France

Received 2 December 2004; accepted 13 December 2004

Abstract

Magnetic and electronic properties of the oxygen deficient ordered perovskite, $Sr_{2/3}Y_{1/3}CoO_{8/3+\delta}$, have been studied for two different oxygen contents corresponding to $\delta = 0.00$ and 0.04 in the chemical formula. For the former, at low temperature, the background state is antiferromagnetic insulating ($T_N = 290\,K$, $\rho_{10\,K} = 4 \times 10^5\,\Omega\,cm$) as expected from the presence of trivalent cobalt in the high spin-state. Remarkably, the more oxidized compound with a cobalt oxidation state of ≈ 3.08 is a ferromagnetic half-metal with $T_C = 225\,K$ and $\rho_{10\,K} = 2 \times 10^{-3}\,\Omega\,cm$. Consistently, upon application of an external magnetic field, the spin-scattering reduction in the T_C vicinity is responsible for a weak negative magnetoresistance. These dramatic changes of the physical properties for such a slight increase of the cobalt oxidation state are interpreted as a result of the structural disordering created by the extra oxygens. The thermoelectric power measurements, showing a sign change of the Seebeck coefficient as the oxygen content increases, indicate that electrons moving in a metallic e_g band dominate the transport properties of the ferromagnetic and metallic compound. This suggests the existence of an orbital ordering in the pristine compound, related to an ordered array of CoO_4 tetrahedra, which can be collapsed by the presence of these extra oxygen anions.

Keywords: Cobaltite; Metal-transition oxide; Nonstoichiometry; Magnetism; Electronic transport; Thermoelectric power; Magnetoresistance; Metal to insulator transition; Cobalt; Spin state

Compared to the charge and orbital degrees of freedom in perovskite manganites, the different spin-states of the cobalt cations provide an additional degree of freedom. For instance, in the case of the $LaCoO_3$ perovskite manganite, the spin-states of the trivalent cobalt in octahedral coordination have been proposed to exhibit thermally assisted spin-state transitions from low spin (LS) to high spin (HS) through intermediate spin (IS) [1]. The change of the cobalt cation ligand field allows also the control of the spin-state. The trivalent cobalt cation in square-plane pyramidal coordination adopts an HS state [2] in contrast to LS in $LaCoO_3$. In this respect, the oxygen deficient $LnBaCo_2O_{5.5}$ perovskite containing trivalent cobalt crystallizes in an interesting ordered structure [3]. For the $O_{5.5}$ stoichiometry, the *A*-site cation ordering favors an oxygen ordering such that the cobalt–oxygen polyhedra form a regular array of CoO_5 square-plane pyramids and CoO_6 octahedra. The spin-state transition for the sixfold coordinated Co^{3+} from HS (or IS) to LS has been proposed to explain the abrupt metal to insulator transition (MIT) occurring in the *T*-region 300 K to 360 K depending on the lanthanide ionic radius [4]. This spin-state transition is believed to create a "spin-blockade" [5]. The electron charge carrier, a high-spin Co^{2+} ($t_{2g}^5 e_g^2$), in the high-*T* state, is delocalized in a broad e_g band made by hybridization through oxygen to its HS (or IS) Co^{3+} neighbors. But as the *T* is sufficiently reduced to make the spin-states of the sixfold Co^{3+} cations evolve towards LS, this HS Co^{2+} becomes trapped, leading to MIT.

*Corresponding author. Fax: +33 2 31 95 16 00.
E-mail address: antoine.maignan@ensicaen.fr (A. Maignan).

0022-4596/$ - see front matter © 2004 Elsevier Inc. All rights reserved.
doi:10.1016/j.jssc.2004.12.014

The search for structures containing regular arrays of different Co^{3+} polyhedra is thus a promising source to discover new electronic and magnetic properties. In that respect the recent report on the $Sr_{1-x}Ln_xCoO_{3-\delta}$ series (Ln = lanthanide), with $0.1 \leqslant x \leqslant 0.5$ and $0.2 \leqslant \delta \leqslant 0.4$, provides a new example of an oxygen-deficient ordered perovskite with both cation (A-site) and oxygen vacancy ordering [6–10]. The crystallographic study of the structures for $x = 0.33$ [8–10] and $x = 0.30$ [6] shows a new type of cation ordering at the A-site, with three different crystallographic sites but only one occupied by Y ($I4/mmm$ space group, $a \approx 2a_{per.}$, $c \approx 4a_{per.}$). The cobalt array can be described as the stacking of one plane of corner-sharing CoO_6 octahedra alternating with a layer made of an original arrangement of the CoO_4 tetrahedra generated by an oxygen vacancy ordering linked to the A-site ordering. For this peculiar ordered perovskite, the magnetic structure is G-type antiferromagnetic with T_N close to room temperature [7–10]. Nevertheless, there is no report about the electronic properties of this ordered perovskite. In this letter, we report on the resistivity, magnetoresistance, thermoelectric power (Seebeck effect, S), thermal conductivity and magnetic measurements of two $Sr_{2/3}Y_{1/3}CoO_{8/3+\delta}$ perovskite cobaltites corresponding to $\delta = 0.00$ and 0.04. Although the superstructure associated to both cation and oxygen vacancy ordering is kept unchanged as probed by the transmission electron microscopy study, a dramatic change of the electronic and magnetic background states is induced by this small oxygen uptake.

The sample has been prepared by mixing the SrO_2, Y_2O_3 and Co_3O_4 precursors in stoichiometric proportions according to the "$Sr_{2/3}Y_{1/3}CoO_x$" formula. The mixtures were ground and then pressed in the form of $2 \times 2 \times 10$ mm bars. The latter were set in finger-like alumina crucibles, which were put in quartz tubes, the latter being then sealed under primary vacuum. The close ampoules were heated in six hours up to 1100 °C and fired for 12 h at this temperature. Finally, the ampoules were quenched in air. In order to increase the oxygen content, the as-prepared bars (abbreviated as-prep. in the following) were post-annealed in oxygen pressure ("PO_2"—samples) at 600 °C for 12 h in 100 atm.

The structural characterizations of these obtained black samples were made by X-ray powder diffraction (XRPD) at room temperature using a Philips diffractometer (Cu$K\alpha$ radiation, $10^\circ \leqslant 2\theta \leqslant 100^\circ$ range, 0.02 step). The XRPD were refined by the Rietveld method (program Fullprof). Samples for transmission electron microscopy (TEM) were crushed in alcohol, and the small flakes were deposited on a holey carbon film, supported by a copper grid. The electron diffraction (ED) study and coupled energy dispersive spectroscopy (EDS) analysis were carried out with a JEOL 200CX electron microscope.

The oxygen content was determined by the thermogravimetric hydrogen reduction method (Ar/H_2 in the 90:10 ratio) using a Setaram TAG 92 microbalance. Iodometric and complexometric titrations were performed to obtain the cobalt oxidation states of the compounds. For both titrations, the end-point is electrochemically determinated by following the potential of the solution with platinum electrodes versus ECS electrode, while the current is held at zero. Each sample (ca. 50 mg) is dissolved in a molar acetic buffer solution (ca. 50 mL) containing an excess of KI (ca. 1 g). Co(+III) and Co(+IV) species are reduced into Co(+II) together with formation of iodine species in stoichiometric amount. Iodine is therefore titrated with $Na_2S_2O_3$ 0.1 N solution using thiodene (starch) as colorimetric indicator in addition to the potential evolution. In order to have access to the global amount of cobalt species in the sample, a complexometric titration is performed; 50 mL of H_2O and 7 mL NH_3 28% is added and titrated with EDTA 0.1 N using murexide as colorimetric indicator.

The resistivity measurements were calculated by using the resistance values measured by the four-point technique. The Seebeck and thermal conductivity were measured by using a steady-state technique. For all the measurements, indium contacts were ultrasonically deposited on the bars. A physical properties measurements system (PPMS, Quantum Design) allowed to measure from 1.8 to 400 K within magnetic fields upon to 7 T. The ac/dc magnetic option of the PPMS and an SQUID magnetometer were used to measure the ac magnetic susceptibility and magnetic moments, respectively.

From the XRPD data, the refined cell parameters of the cell for the as-prep. and those of the PO_2 samples remain very similar ($I4/mmm$), [$a = 0.7618$ nm, $c = 1.5314$ nm] and [$a = 0.7614$ nm, $c = 1.5317$ nm] for the former and latter, respectively. The refinements show also a good agreement with the nominal "$Sr_{2/3}Y_{1/3}Co$" cation stoichiometry and this is also confirmed for both samples by EDS analyses coupled to electron diffraction performed before and after the PO_2 annealing. These results combined to the oxygen stoichiometry determined from the TGA curves and the chemical titrations (Table 1) yield the following formulas, $Sr_{2/3}Y_{1/3}CoO_{2.66}$ and $Sr_{2/3}Y_{1/3}CoO_{2.70}$ for the as-prep. and PO_2 samples, respectively. From these chemical studies, the calculated cobalt oxidation states are ~3.00 and ~3.08 for the as-prep. and PO_2 samples, respectively. Nevertheless, as shown in the following, this slight increase of the oxygen content affects strongly the physical properties.

A first effect is seen on the T dependent resistivity curves (Fig. 1). Though the absolute values at the highest temperature are almost the same, $\rho \sim 4$ mΩ cm, the $(d\rho/dT)$ coefficient goes from negative to positive as

Table 1
Oxidation states of the cobalt cations calculated from the oxygen content values determined by using titration and TGA measurements for the $Sr_{2/3}Y_{1/3}CoO_{3-\delta}$ (as-prep.) and post-annealed samples (PO_2)

Samples	Oxidation degree for Co	δ in $Sr_{2/3}Y_{1/3}CoO_{2\cdot66+\delta}$ from titration	δ in $Sr_{2/3}Y_{1/3}CoO_{2\cdot66+\delta}$; from TGA
As-prep.	2.99	0.00	0.01
PO_2 annealed	3.08	0.05	0.04

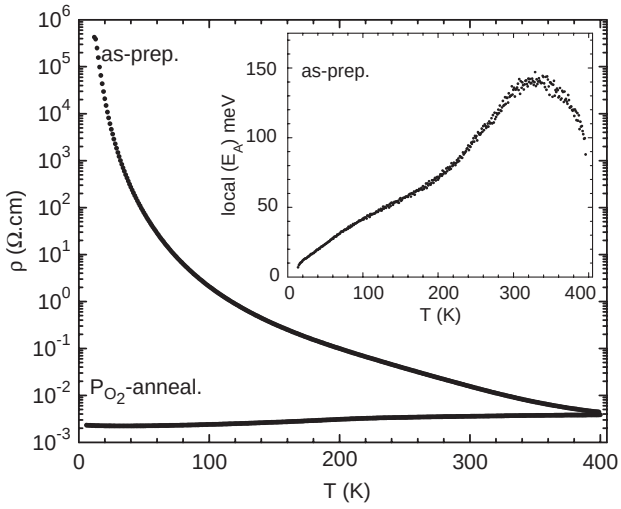

Fig. 1. T-dependent resistivity (ρ) of $Sr_{2/3}Y_{1/3}CoO_{2.66}$ (as-prep.) and $Sr_{2/3}Y_{1/3}CoO_{2.70}$ (PO_2) samples. Inset: corresponding local activation energy as a function of T for the as-prep. sample.

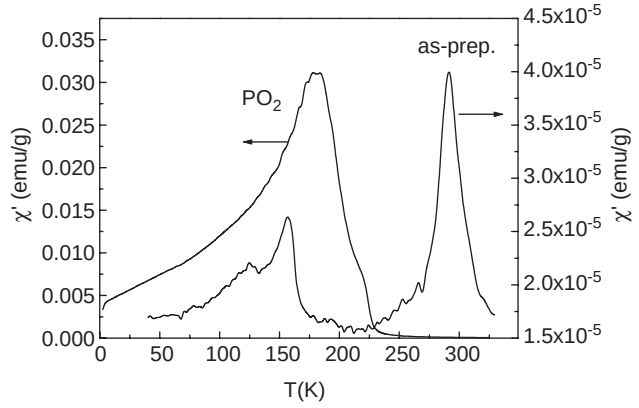

Fig. 2. T-dependent ac magnetic susceptibility (real part, χ') of the as-prep. (right y-axis) and PO_2 (left y-axis) samples.

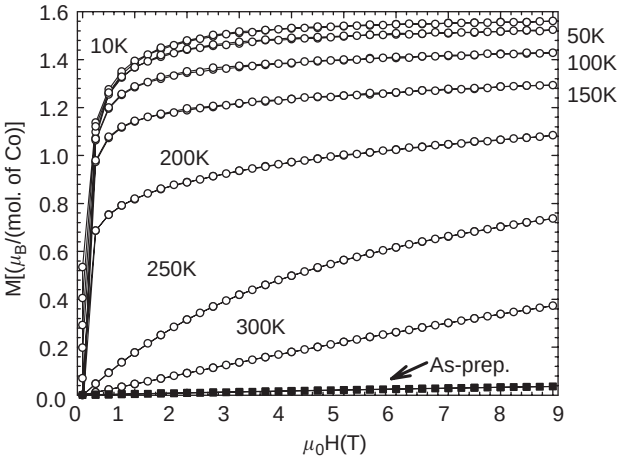

Fig. 3. Isothermal magnetic field dependence (H) of the magnetization (M) for the $Sr_{2/3}Y_{1/3}CoO_{2.66}$ (as-prep., filled squares, $T = 10\,K$) and $Sr_{2/3}Y_{1/3}CoO_{2.70}$ (PO_2, empty circles) samples.

one gives from the as-prep. to the PO_2 sample. For instance for the lowest T values, the $\rho_{10\,K}$ values are $4 \times 10^5\,\Omega$cm and $2\,m\Omega$cm for the as-prep. and PO_2 samples, respectively. Thus, at this temperature the ρ change is of ~8 orders of magnitude. Furthermore, these curves exhibit slope changes. This is clearly visible on the $\rho(T)$ curve at ~210 K for the PO_2 sample, whereas the slope change at about ~300 K on the $\rho(T)$ curve of the as-prep. compound is more easily observed on the T-dependent local activation energy, $E_{A(local)} = k(d \ln \rho / dT^{-1})$, where k is the Boltzman constant (inset of Fig. 1).

These very different electronic properties reflect a strong change in the magnetic properties. As previously reported, the T dependence of the ac $-\chi$ for the $O_{2.66}$ as-prep. sample shows a clear maximum at ~300 K (Fig. 2) which corresponds to the antiferromagnetic Néel temperature as probed by neutron powder diffraction [10]. In comparison, the ac $-\chi$ values of the PO_2 sample, larger by almost ~3 orders magnitude, show a sharp χ increase below about ~225 K (Fig. 2). To check further the magnetic behavior, the magnetic field (H) dependence of the magnetization (M) was measured (Fig. 3). For the as-prep. sample, the $M(H)$ curve reveals low M values consistent with the antiferromagnetic state. In contrast, the $M(H)$ data for the PO_2 sample are typical of ferromagnetism, with an M saturation and an hysteresis around $H = 0$. The M values, reaching up to ~1.6μ_B per mole of cobalt, are large and must be compared to the value of the saturation magnetization, M_S~2μ_B, reported for $La_{0.5}Sr_{0.5}CoO_3$ [1] and $SrCoO_3$ [11], i.e., cobalt oxidation states in the range of 3.5–4. To sum up, the post-annealing under oxygen pressure of the as-prepared compound makes increasing the cobalt oxidation from ~3.00 to ~3.08 for the PO_2 sample.

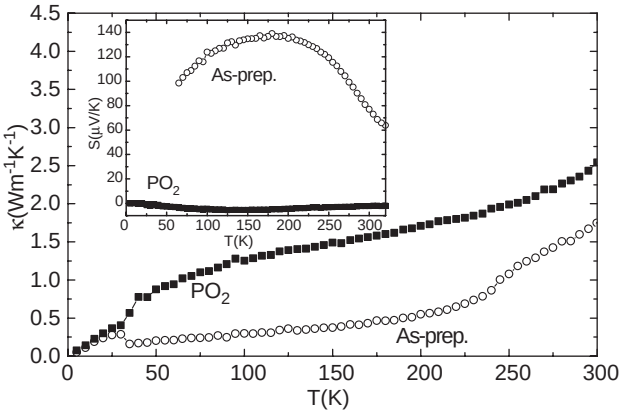

Fig. 4. T dependent thermal conductivity (κ) of the as-prep. and PO_2 samples. Inset: T-dependent Seebeck coefficient (S) for the as-prepared (as-prep.) and oxygen pressure annealed (PO_2) samples; note that the values for the as-prep. sample were not measurable for $T \leqslant 50$ K due to the too large sample resistance at low T (see the $\rho(T)$ curve in Fig. 1).

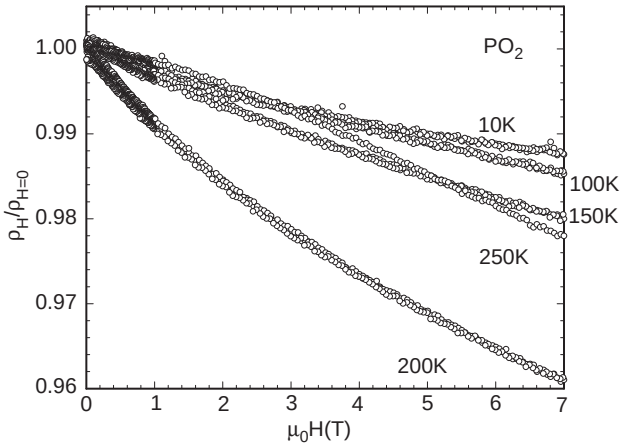

Fig. 5. Isothermal magnetic field (H) dependence of the normalized resistivity for the PO_2 sample.

The electronic and magnetic background state is dramatically changed evolving from antiferromagnetic insulating to ferromagnetic metallic.

In order to test the nature of the charge carriers, Seebeck (S) measurements as a function of T have been performed (inset of Fig. 4). For the as-prep. sample, the S values are positive and large; for instance, at $T = 300$ K, S is equal to $+60\,\mu V\,K^{-1}$. These data, reflecting the hole nature of the charge carriers, are comparable to those reported for $x = 0.10$ in the $La_{1-x}Sr_xCoO_3$ series [1]. The corresponding cobalt oxidation state of 3.1 is thus slightly larger than the calculated value from the chemical formula. The $S(T)$ curve of the PO_2 sample is very different, showing a negative TEP with small absolute values. The $S_{300\,K}$ value, $-2\,\mu V\,K^{-1}$, is very similar to that reported for the metallic $SrCoO_3$ perovskite [11]. For the PO_2 sample, the calculated cobalt oxidation state, 3.08, cannot be simply compared to the $v_{Co} = 4$ value of $SrCoO_3$ which exhibits same S values. The bulk character of the insulator to metal transition induced by post-annealing is also confirmed by the increase of the thermal conductivity (Fig. 4) from $\kappa_{300\,K} = 1.75\,WK^{-1}\,m^{-1}$ to $\kappa_{300\,K} = 2.25\,WK^{-1}\,m^{-1}$ as the oxygen content goes from $O_{2.66}$ to $O_{2.70}$. Furthermore, a clear bump is observed at about 250 K on the $\kappa(T)$ curve of the as-prep. compound so that the κ values become smaller below 250 K; for instance, κ values are 0.7 and $1.5\,W\,K^{-1}\,m^{-1}$ at 225 and 275 K. This κ decrease is consistent with the $\chi(T)$ data (Fig. 2) showing that in this T region the antiferromagnetic transition is completed. It shows clearly that in this as-prep. sample the antiferromagnetic state is less conducting than the paramagnetic one.

These different magnetic and electronic states suggest different magnetoresistance properties for the as-prep. and PO_2 samples. As shown in Fig. 5, the PO_2 sample exhibits negative MR values [$MR = 100x((\rho_H - \rho_{H=0})/\rho_{H=0})$], $\sim -4\%$ in a magnetic field of 7 T for $T \sim 200$ K, i.e., in the T_C vicinity, whereas the as-prep. sample shows a negative magnetoresistance of only -1% in 7 T at 10 K. For the ferromagnetic PO_2 sample, upon magnetic field application, the reduction of the spin scattering is responsible for the observed negative MR.

The evolution of the present properties for the $Sr_{2/3}Y_{1/3}CoO_{3-\delta}$ samples, as the content of oxygen vacancy goes from $\delta = 1/3$ to 0.30, is very unexpected, especially as one compares them to those of the oxygen stoichiometric $La_{1-x}Sr_xCoO_3$ perovskite. For the same formal cobalt oxidation states the properties are very different. The first difference concerns the antiferromagnetic state, with a high T_N of $\sim$300 K for $Sr_{2/3}Y_{1/3}CoO_{2.66}$ [10], to be compared to the paramagnetic behavior of $LaCoO_3$, i.e., containing also almost pure trivalent cobalt. For the latter, the magnetic behavior is linked to the fact that the Co^{3+} spin state, at low T, is LS ($S = 0$) and then evolves towards higher spin-states as T increases. This suggests strongly that the presence of CoO_4 tetrahedra in the $Sr_{2/3}Y_{1/3}CoO_{2.66}$ structure favors higher spin-states for the cobalt cations, as evidenced by the magnetic moments on each cobalt in the antiferromagnetic structure [10]. The higher spin state for Co^{3+}, IS or HS, in $Sr_{2/3}Y_{1/3}CoO_{2.66}$ is consistent with the high spin state reported in the case of the $Sr_2Co_2O_5$ brownmillerite which structure exhibits also stacking of planes of edge-shared CoO_6 octahedra with planes of CoO_4 tetrahedra [11–13].

The existence of the antiferromagnetic arrangement of the cobalt magnetic moments on the cobalt array in $Sr_{2/3}Y_{1/3}CoO_{2.66}$ creates a strong localization of the charge carriers. For that background state, the thermal excitations are supposed to favor the charge hopping of

holes if one considers the positive Seebeck. Remarkably, a small re-filling of the oxygen vacancies to reach an oxygen stoichiometry of $O_{2.70}$ is sufficient to transform the background state to ferromagnetic metal. The extra oxygens, inserted at the level of the tetrahedra layer, create new bridging between cobalt neighbors which coordination is changed from fourfold to fivefold (or sixfold). The resulting disorder appears to be sufficient to collapse the ordered structure. Such a result is very similar to the substituting effects in orbitally/charge order manganites [14]. The impurity substituted for manganese (at a level of ~1%) can be sufficient to prevent the establishment of the orbital/charge ordered structure. This allows to reveal the underlying ferromagnetic state. This scenario could also hold for the ordered $Sr_{2/3}Y_{1/3}CoO_{2.66}$ oxygen deficient cobaltite. Both antiferromagnetism and ferromagnetism are competing, and the great sensitivity of the former to the oxygen disordering suggests that there exists an orbital ordering to which the antiferromagnetic structure is connected.

The disorder induced ferromagnetism is also very unusual for a cobaltite with such a cobalt oxidation state: in the $La_{1-x}Sr_xCoO_3$ series, the ferromagnetism for $x \sim 0.10$ is associated to the hole nature of the charge carriers moving in a conduction band of mixed t_{2g}/e_g character. For the $Sr_{2/3}Y_{1/3}CoO_{2.70}$ cobaltite, since the structure favors the stabilization of higher spin states, the e_g character is reinforced. The situation becomes thus similar to the metallic ferromagnetism of $SrCoO_3$ [11]. The itinerant electrons in the e_g band are coupled with the more localized t_{2g} ones so that ferromagnetism is induced. Since a pure Co^{3+} HS state ($S = 2$) would lead to a saturation magnetization of $\sim 4\mu_B$ to be compared to a measured value of $1.7\mu_B$, the cobalt spin state is either lower (IS, $S = 1$; $M_S = 2\mu_B$) or the different cobalt sites show different spin-states which combination yields the measured value. The formation of an e_g broadband has been also proposed to explain both small absolute value of the negative S and metallic behavior for $LnBaCo_2O_{5.5}$ [5]. For this compound, at high enough T the thermal excitations create some holes and electrons following the equilibrium: $2Co^{3+} \leftrightarrow Co^{2+} + Co^{4+}$. According to our previous study of this Co^{3+} cobaltite, and since Co^{2+} is mainly high-spin, an electron can move in the e_g band if its Co^{3+} neighbors are in an HS (or IS) state whereas they are "blocked" in the case of LS Co^{3+}, due to incompatible spin state configurations. For the PO_2-annealed sample, the HS (or IS) states configurations of the Co^{3+} species, favored by the presence in the adjacent planes of CoO_4 tetrahedra, which elongate the CoO_6 octahedra, are compatible with a metallic behavior. The magnetic coupling between delocalized e_g electrons and more localized t_{2g} ones favors a ferromagnetic state. The difference with the $La_{1-x}Sr_xCoO_3$ series comes thus from their different Co^{3+} spin-states resulting from different ligand fields in the octahedra. The most intriguing point concerns the origin of the ferromagnetic metallic state, which can be easily induced by the uptake of oxygens. The ordering of the oxygen array in 1 layer over 2 creates a peculiar ordering of the CoO_4 tetrahedra. If only tetrahedra were present, the oxygen stoichiometry would be $O_{2.50}$. In the adjacent planes of elongated $Co^{3+}O_6$ octahedra ($d_{eq.} = 1.91$ Å and $d_{ap.} = 2.08$ Å ref. [6]) the HS Co^{3+} spin state is favored. According to the Goodenough and Kanamori rules [15], the resulting in-plane superexchange is predicted to be strongly antiferromagnetic. For $O_{2.66}$, the oxygen excess of 0.16, creates locally cobalt cations in a fivefold or sixfold coordination. According to ref. [6,7], the extra oxygen to go from $O_{2.5}$ to $O_{2.66}$ are distributed in a disordered manner in the structure. This probably creates new Co–O–Co magnetic coupling which could be ferromagnetic. Nevertheless, the sample is antiferromagnetic, but, from neutron powder diffraction experiments, the net magnetic moment per cobalt is only $2\mu_B$ per cobalt [10], i.e., close to the measured value ($1.7\mu_B$). In that case, the trivalent cobalt cations could be thus in the intermediate spin-state. This may explain that an orbital ordered structure is obtained with d_z2 orbitals along the elongation direction of the octahedra (see Fig. 6). After the oxygen post-annealing, which makes increasing the oxygen content from $O_{2.66}$ to $O_{2.70}$, the additional $J > O$ magnetic exchange interactions frustrate the $J < O$ magnetic exchange coupling. The introduction of extra oxygen anions in the separating layer will tend to locally decrease the CoO_6 distortion of the CoO_6 neighbor so that the e_g orbital degeneracy will

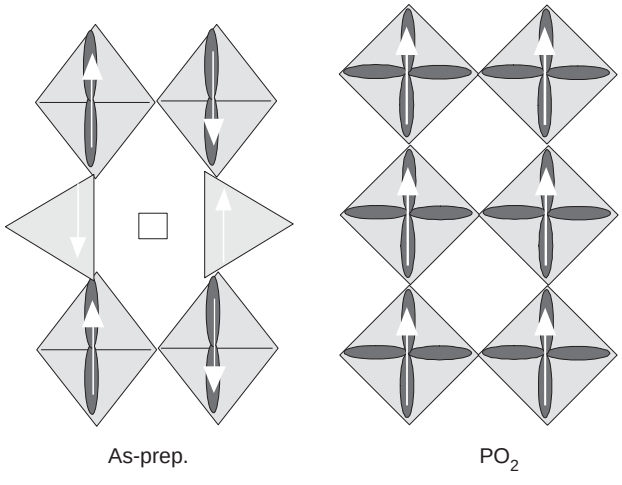

Fig. 6. Schematic drawings showing the orbitals and spins in the as-prep. $Sr_{2/3}Y_{1/3}CoO_{2.66}$ (left) and PO_2-annealed $Sr_{2/3}Y_{1/3}CoO_{2.70}$ (right) samples. The d_z2 orbitals (IS Co^{3+}) in the elongated octahedra are ordered in the $O_{2.66}$ sample leading to the antiferromagnetic insulating state. The refilling of the oxygen vacancies (symbolized as a square in the left) leads to the orbital disordering (right) responsible for the ferromagnetic metallic state.

be restored (Fig. 6). This e_g orbitals disordering makes locally the exchange ferromagnetic instead of antiferromagnetic.

Finally, considering the strong ferromagnetic state experimentally observed for the $O_{2.70}$ sample, one can propose that the orbital disordering induced by extra oxygens added in the orbital ordered structure of $Sr_{2/3}Y_{1/3}CoO_{8/3}$ is responsible for the formation of an e_g broadband in which Co^{2+} electrons are delocalized and polarize ferromagnetically the t_{2g} spins.

References

[1] M.A. Senaris-Rodriguez, J.B. Goodenough, J. Solid State Chem. 118 (1995) 323.
[2] Z. Hu, et al., Phys. Rev. Lett. 92 (2004) 207402.
[3] C. Martin, A. Maignan, D. Pelloquin, N. Nguyen, B. Raveau, Appl. Phys. Lett. 71 (1997) 1421.
[4] A. Maignan, C. Martin, D. Pelloquin, N. Nguyen, B. Raveau, J. Solid State Chem. 142 (1999) 247.
[5] A. Maignan, V. Caignaert, B. Raveau, D. Khomskii, G. Sawatzky, Phys. Rev. Lett. 93 (2004) 026401.
[6] S.Ya. Istomin, J. Grins, G. Svensson, O.A. Drozhzhin, V.L. Kozhevnikov, E.V. Antipov, J.P. Attfield, Chem. Mater. 15 (2003) 4012.
[7] S.Ya. Istomin, O.A. Drozhzhin, G. Svensson, E.V. Antipov, Solid State Sci. 6 (2004) 539.
[8] R.L. Withers, M. James, D.J. Goossens, J. Solid State Chem. 174 (2003) 198.
[9] M. James, D. Cassidy, D.J. Goossens, R.L. Withers, J. Solid State Chem. 177 (2004) 1886.
[10] D.J. Goossens, K.F. Wilson, M. James, A.-J. Studer, X.L. Wang, Phys. Rev. B 69 (2004) 134411.
[11] P. Bezdicka, A. Wattiaux, J.C. Grenier, M. Pouchard, P. Haguenmuller, Z. anorg. Allg. Chem. 619 (1993) 7.
[12] T. Takeda, Y. Yamaguchi, H. Watanabe, J. Phys. Soc. Jpn. 33 (1972) 970.
[13] F. Lindberg, S. Ya. Istomin, P. Berastegui, G. Svensson, S.M. Kazakov, E.V. Antipov, J. Solid State Chem. 173 (2003) 395.
[14] B. Raveau, A. Maignan, C. Martin, J. Solid State Chem. 130 (1997) 162.
[15] J.B. Goodenough, A. Wold, R.J. Arnot, N. Menyuk, Phys. Rev. B 124 (1961) 373.